

Ramping fermions in optical lattices across a Feshbach resonance

Helmut G. Katzgraber, Aniello Esposito, and Matthias Troyer
Theoretische Physik, ETH Zürich, CH-8093 Zürich, Switzerland

(Dated: November 11, 2018)

We study the properties of ultracold Fermi gases in a three-dimensional optical lattice when crossing a Feshbach resonance. By using a zero-temperature formalism, we show that three-body processes are enhanced in a lattice system in comparison to the continuum case. This poses one possible explanation for the short molecule lifetimes found when decreasing the magnetic field across a Feshbach resonance. Effects of finite temperatures on the molecule formation rates are also discussed by computing the fraction of double-occupied sites. Our results show that current experiments are performed at temperatures considerably higher than expected: lower temperatures are required for fermionic systems to be used to simulate quantum Hamiltonians. In addition, by relating the double occupancy of the lattice to the temperature, we provide a means for thermometry in fermionic lattice systems, previously not accessible experimentally. The effects of ramping a filled lowest band across a Feshbach resonance when increasing the magnetic field are also discussed: fermions are lifted into higher bands due to entanglement of Bloch states, in good agreement with recent experiments.

PACS numbers: 03.75.Ss, 05.30.Fk, 71.10.Ca

I. INTRODUCTION

Ultracold atoms loaded into optical lattices are nearly ideal experimental realizations of nonrelativistic quantum lattice models [1]. Experiments on bosonic atoms in optical lattices have demonstrated the transition from superfluid to Mott insulator states [2], and probed momentum distribution and excitation spectra in strongly interacting bosonic systems [3, 4]. Comparisons to quantum Monte Carlo [5, 6, 7, 8, 9] and density matrix renormalization group calculations [10] exhibit good quantitative agreement and confirm the quantitative applicability of simple quantum lattice models to describe atomic gases in optical lattices. Bosons in optical lattices thus provide an interesting test bed for theoretical models, such as the recently introduced ring-exchange model [11].

In contrast to bosonic systems, the physics of strongly interacting *fermions* in two- and three-dimensional lattices is not yet fully understood. Indeed, accurate numerical simulations on interacting fermionic systems in two- and three-dimensional lattice models are nondeterministic polynomial hard [12], and no general numerical or analytical solution exists. Experiments on ultracold fermionic gases in optical lattices could thus be very useful in elucidating the properties of the fermionic Hubbard model [13, 14] and to probe exotic quantum phases, such as *d*-wave resonating valence bond phases [15].

Progress in cooling techniques for fermionic atoms has recently allowed the first experiments on cold *fermionic* gases in optical lattices to be performed by T. Esslinger and coworkers [16, 17, 18]. In a first experiment they loaded a weakly interacting cold Fermi gas into an optical lattice and observed the momentum distribution function. Ramping this Fermi gas across a Feshbach resonance by increasing the magnetic field has been seen to lift a fraction of the atoms into higher bands. In a second experiment, the atoms were ramped across the Feshbach resonance by decreasing the magnetic field, which leads

to the formation of molecules [19].

In this paper we present analytical and numerical calculations on fermions in three-dimensional optical lattices to quantitatively explain the experiments of Köhl *et al.* [16] when ramping up the field. We start in Sec. II with a calculation of the two- and three-particle densities in optical lattices to compare loss rates in the continuum to lattices. Next we consider the effects of finite temperatures in Sec. III and relate the double occupancy in the lattice to the temperature of the system, thus providing a means for thermometry [20] in fermionic experiments. Our results show that at experimentally accessible temperatures, the double occupancy of lattice sites is substantially reduced compared to the ground state; this has important consequences for the quantitative explanation of the experiments of Ref. [16], discussed in Sec. IV.

II. TWO- AND THREE-PARTICLE DENSITIES

We start by solving the Schrödinger equation for non-interacting fermions in an optical lattice, in order to compute the two- and three-particle densities.

A. Schrödinger equation

Superimposing two counterpropagating running-wave laser beams of wavelength $\lambda = 2\pi/k$ (k is the wave vector) in all three spatial directions yields a static potential $U(\mathbf{r})$ with periodicity $a = \lambda/2$:

$$U(\mathbf{r}) = \sum_{i=1}^3 U \sin^2(k_i x_i), \quad (1)$$

where $\mathbf{r} = (x_1, x_2, x_3)$. We consider a cubic system with N^3 sites, and a linear extent $L = aN$. In or-

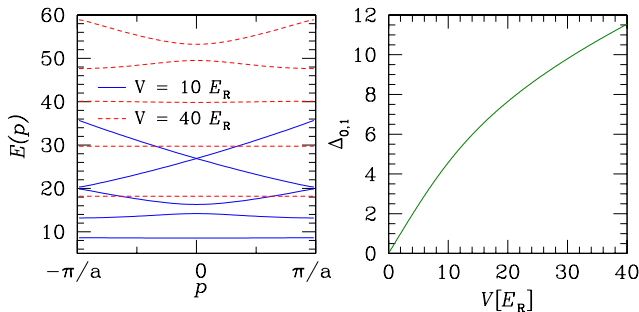


FIG. 1: (Color online) Left: Five lowest bands in the first Brillouin zone plotted as a function of the wave vector $\mathbf{p} = (p, 0, 0)$ for $V = 10$ (solid lines) and 40 (dashed lines). Right: Band gap $\Delta_{0,1}$ between the lowest and first excited bands as a function of the potential V in units of E_R .

der to describe fermions in an optical lattice, the time-independent Schrödinger equation

$$\left[-\frac{\hbar^2}{2m} \nabla^2 + U(\mathbf{r}) \right] \Psi(\mathbf{r}) = E\Psi(\mathbf{r}), \quad (2)$$

has to be solved for each spin state. Here m represents the atomic mass. Using a product ansatz $\Psi(\mathbf{r}) = \psi_1(x_1)\psi_2(x_2)\psi_3(x_3)$ with $E = E_1 + E_2 + E_3$, each component can be solved via Bloch states

$$\psi_{i,n_i,p_i}(x_i) = e^{ip_i x_i} u_{n_i,p_i}(x_i) \quad (3)$$

with periodic functions

$$u_{n_i,p_i}(x_i + a) = u_{n_i,p_i}(x_i) \quad (4)$$

and corresponding energy eigenvalues E_{n_i,p_i} . Here $n_i \in \mathbb{N}$ is the band index and $p_i \in \mathbb{R}$ the quasimomentum. In order to describe finite lattices, we impose periodic boundary conditions [$\psi_{i,n_i,p_i}(x_i) = \psi_{i,n_i,p_i}(x_i + L)$] to the solution, yielding a discrete set of N allowed quasimomenta $p_i = -\pi/a, -\pi/a + 2\pi/L \dots, \pi/a - 2\pi/L$ in the first Brillouin zone (first BZ) given by the interval $(-\pi/a, \pi/a)$. A full three-dimensional Bloch state $\Psi_{\mathbf{n},\mathbf{p}}$ is thus parametrized by two vectors $\mathbf{n} = (n_1, n_2, n_3)$ and $\mathbf{p} = (p_1, p_2, p_3)$, as well as its energy $E_{\mathbf{n},\mathbf{p}} = E_{n_1,p_1} + E_{n_2,p_2} + E_{n_3,p_3}$, where each band carries N^3 allowed states for each spin state. Figure 1, left panel, shows the five lowest bands for $V = U/E_R = 10$ and 40, where $E_R = \hbar^2 k^2 / 2m$. The right panel of Fig. 1 shows the band gap $\Delta_{0,1}$ between the ground state and first excited state as a function of the potential V . Inserting Eq. (3) into Eq. (2), we obtain

$$\left[\frac{1}{k^2} \left(-\frac{\partial^2}{\partial x^2} - 2ip \frac{\partial}{\partial x} + p^2 \right) + V \sin^2(kx) \right] u_{n,p}(x) \quad (5)$$

$$= \epsilon_{n,p} u_{n,p}(x).$$

In Eq. (5) we have expressed the potential U in units of the recoil energy $E_R = \hbar^2 k^2 / 2m$, i.e., $V = U/E_R$ and

$\epsilon_{n,p} = E_{n,p}/E_R$. We solve Eq. (5) with a Fourier ansatz for periodic functions

$$u_{n,p}(x) = \lim_{c \rightarrow \infty} \sum_{j=-c}^{+c} \bar{u}_{n,p,j} e^{ijx2\pi/a}, \quad (6)$$

$$\bar{u}_{n,p,j} = \frac{1}{a} \int_{-a/2}^{a/2} e^{ijx2\pi/a} u_{n,p}(x) dx. \quad (7)$$

Note that in Eqs. (6) and (7) we introduce a cutoff c . If we consider only the lowest five bands $\epsilon_{n,p}$, $n = 1, \dots, 5$, convergence beyond machine precision is attained already for $c = 6$.

B. Two- and three-particle densities

Experimentally, molecule formation rates [16] have not been as high as expected. This can be attributed either to temperature fluctuations or to three-body processes hampering the molecule formation. Naively one would expect that increasing the potential depth V would suppress three-body processes disrupting molecule formation. In order to test this, we compute the three particle density and show that at moderate potential depths V , in a range relevant for experiments, it is actually larger than without an optical lattice.

To calculate the probability of having three fermions in a small volume, we start with a filled lowest band $\mathbf{n} = \mathbf{n}_0 \equiv (0, 0, 0)$, i.e., each site carries two particles with opposite spin states. The ground state $|\Phi_0\rangle$ is then given by

$$|\Phi_0\rangle \equiv \prod_{\mathbf{p} \in \text{first BZ}} \hat{a}_{\mathbf{n}_0, \mathbf{p}, \uparrow}^\dagger \hat{a}_{\mathbf{n}_0, \mathbf{p}, \downarrow}^\dagger |0\rangle \quad (8)$$

where $\hat{a}_{\mathbf{n}, \mathbf{p}, s}^\dagger$ ($\hat{a}_{\mathbf{n}, \mathbf{p}, s}$) creates (annihilates) a particle in a Bloch state $|\Psi_{\mathbf{n}, \mathbf{p}}\rangle$ with spin $s \in \{\uparrow, \downarrow\}$. The product over \mathbf{p} is carried out over the allowed states in the first Brillouin zone. The corresponding field operators defined in terms of Bloch states are given by

$$\hat{\Psi}_s(\mathbf{r}) \equiv \sum_{\mathbf{n}, \mathbf{p}} \Psi_{\mathbf{n}, \mathbf{p}}(\mathbf{r}) \hat{a}_{\mathbf{n}, \mathbf{p}, s},$$

$$\hat{\Psi}_s^\dagger(\mathbf{r}) \equiv \sum_{\mathbf{n}, \mathbf{p}} \Psi_{\mathbf{n}, \mathbf{p}}^*(\mathbf{r}) \hat{a}_{\mathbf{n}, \mathbf{p}, s}^\dagger, \quad (9)$$

where the summation is carried out over all band indices $\mathbf{n} \in \mathbb{N}_0^3$ and allowed \mathbf{p} in the first Brillouin zone. The three-particle density ρ_3 in a small volume at a given lattice site is then given by

$$\rho_3(\mathbf{r}, \mathbf{r}') \equiv \langle \Phi_0 | \hat{\Psi}_\uparrow^\dagger(\mathbf{r}) \hat{\Psi}_\downarrow^\dagger(\mathbf{r}) \hat{\Psi}_\uparrow^\dagger(\mathbf{r}') \hat{\Psi}_\uparrow(\mathbf{r}') \hat{\Psi}_\downarrow(\mathbf{r}) \hat{\Psi}_\uparrow(\mathbf{r}) | \Phi_0 \rangle, \quad (10)$$

where we have one up and one down spin at position \mathbf{r} , and one up spin at position \mathbf{r}' . The operators $\hat{\Psi}_s^\dagger(\mathbf{r})$

$[\widehat{\Psi}_s(\mathbf{r})]$ create (annihilate) a particle with spin state $s \in \{\uparrow, \downarrow\}$ at a space point \mathbf{r} . These can be inserted into

Eq. (10). After a straightforward derivation one obtains for the three-particle density

$$\rho_3(\mathbf{r}, \mathbf{r}') = \sum_{\mathbf{p}_1, \mathbf{p}_2, \mathbf{p}_3} [|\Psi_{\mathbf{n}_0, \mathbf{p}_1}(\mathbf{r})|^2 |\Psi_{\mathbf{n}_0, \mathbf{p}_2}(\mathbf{r})|^2 |\Psi_{\mathbf{n}_0, \mathbf{p}_3}(\mathbf{r})|^2 - \Psi_{\mathbf{n}_0, \mathbf{p}_1}^*(\mathbf{r}) \Psi_{\mathbf{n}_0, \mathbf{p}_1}(\mathbf{r}') |\Psi_{\mathbf{n}_0, \mathbf{p}_2}(\mathbf{r})|^2 \Psi_{\mathbf{n}_0, \mathbf{p}_3}^*(\mathbf{r}') \Psi_{\mathbf{n}_0, \mathbf{p}_3}(\mathbf{r})]. \quad (11)$$

Flipping the signs of the spins at \mathbf{r} and \mathbf{r}' in Eq. (10) does not affect the expression in Eq. (11).

The two-particle density ρ_2 for two atoms in the *same* spin state is given by

$$\rho_2(\mathbf{r}, \mathbf{r}') \equiv \langle \Phi_0 | \widehat{\Psi}_\uparrow^\dagger(\mathbf{r}') \widehat{\Psi}_\uparrow^\dagger(\mathbf{r}) \widehat{\Psi}_\uparrow(\mathbf{r}) \widehat{\Psi}_\uparrow(\mathbf{r}') | \Phi_0 \rangle, \quad (12)$$

and can be evaluated in a similar way as Eq. (10):

$$\rho_2(\mathbf{r}, \mathbf{r}') = \sum_{\mathbf{p}_1, \mathbf{p}_2} [|\Psi_{\mathbf{n}_0, \mathbf{p}_1}(\mathbf{r}')|^2 |\Psi_{\mathbf{n}_0, \mathbf{p}_2}(\mathbf{r})|^2 - \Psi_{\mathbf{n}_0, \mathbf{p}_1}^*(\mathbf{r}') \Psi_{\mathbf{n}_0, \mathbf{p}_1}(\mathbf{r}) \Psi_{\mathbf{n}_0, \mathbf{p}_2}^*(\mathbf{r}) \Psi_{\mathbf{n}_0, \mathbf{p}_2}(\mathbf{r}')]. \quad (13)$$

Finally, we compute the probability ρ_2° of finding two fermions in opposite spin states at positions \mathbf{r} and \mathbf{r}'

$$\rho_2^\circ(\mathbf{r}, \mathbf{r}') \equiv \langle \Phi_0 | \widehat{\Psi}_\uparrow^\dagger(\mathbf{r}') \widehat{\Psi}_\downarrow^\dagger(\mathbf{r}) \widehat{\Psi}_\downarrow(\mathbf{r}) \widehat{\Psi}_\uparrow(\mathbf{r}') | \Phi_0 \rangle \quad (14)$$

which can also be expressed as

$$\rho_2^\circ(\mathbf{r}, \mathbf{r}') = \sum_{\mathbf{p}_1, \mathbf{p}_2} [|\Psi_{\mathbf{n}_0, \mathbf{p}_1}(\mathbf{r}')|^2 |\Psi_{\mathbf{n}_0, \mathbf{p}_2}(\mathbf{r})|^2]. \quad (15)$$

Because of the short-range nature of the three-body interactions, we are most interested in the limit $|\mathbf{r} - \mathbf{r}'| \rightarrow 0$. Since both ρ_2 and ρ_3 vanish in that limit due to the Pauli principle, we calculate their average over a small volume Ω_R ($a/2 \leq R \leq a/32$) around the origin

$$\bar{\rho}(V) \equiv \frac{1}{|\Omega_R|} \int_{\Omega_R} \rho(0, \mathbf{r}') d\mathbf{r}'. \quad (16)$$

In Fig. 2 we show data for the averaged two- and three-particle densities according to Eq. (16) as a function of the potential depth V . The data show a marked peak that exceeds unity for moderate potential depths. This leads to three-particle processes that in turn lead to molecular loss in the fermion gas. For large potential depths both densities are exponentially suppressed. This is in contrast to a configuration with only two fermions having different spins, as can be seen by divergence of $\bar{\rho}_2^\circ$ in Fig. 2.

C. Partially filled lowest bands at zero temperature

So far we have not taken into account the Gaussian-shaped intensity profile of the lasers generating the optical lattice which yields a superimposed harmonic confinement [21]. The inhomogeneity of the trapping potential

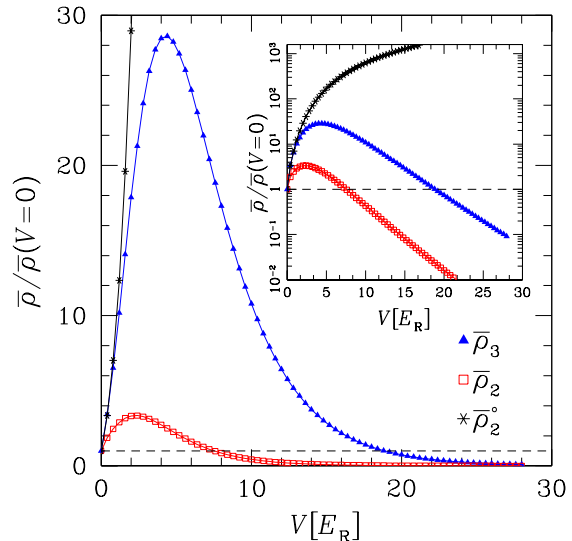


FIG. 2: (Color online) Averaged three-particle density $\bar{\rho}_3(V)$ and average two-particle density $\bar{\rho}_2(V)$ via Eq. (16) as a function of the optical potential depth V calculated on cubes of linear extent $R = a/32$ in lattices with $N = 65$. The graphs are normalized in such a way that $\bar{\rho}_3(V=0) = 1$ (free fermion gas). The dashed horizontal line marks where the densities cross unity. As shown in the inset, for a completely filled lowest band and $V \gtrsim 6$, the probability of finding two particles per site in the same spin state is exponentially suppressed, whereas the probability of finding two fermions in different spin states, $\bar{\rho}_2^\circ(V)$, diverges.

influences the spatial density distribution of the particles in the lattice. The effects of the trapping potential are often considered in a “local density” approximation, where the local properties in the trap are approximated by results obtained from a homogeneous system with the same local density.

The partially filled ground state in terms of Bloch states is given by

$$|\Phi_0\rangle \equiv \prod_{\mathbf{p} \in \Lambda} \widehat{a}_{\mathbf{n}_0, \mathbf{p}, \uparrow}^\dagger \widehat{a}_{\mathbf{n}_0, \mathbf{p}, \downarrow}^\dagger |0\rangle, \quad (17)$$

where Λ is the region of the first Brillouin zone inside the Fermi surface. We can again compute the three-particle density now restricted to momenta inside Λ and obtain

$$\rho_3(\mathbf{r}, \mathbf{r}') = \sum_{\mathbf{p}_1, \mathbf{p}_2, \mathbf{p}_3} \chi_\Lambda(\mathbf{p}_1) \chi_\Lambda(\mathbf{p}_2) \chi_\Lambda(\mathbf{p}_3) \left[|\Psi_{\mathbf{n}_0, \mathbf{p}_1}(\mathbf{r})|^2 |\Psi_{\mathbf{n}_0, \mathbf{p}_2}(\mathbf{r})|^2 |\Psi_{\mathbf{n}_0, \mathbf{p}_3}(\mathbf{r})|^2 \right. \\ \left. - \Psi_{\mathbf{n}_0, \mathbf{p}_1}^*(\mathbf{r}) \Psi_{\mathbf{n}_0, \mathbf{p}_1}(\mathbf{r}') |\Psi_{\mathbf{n}_0, \mathbf{p}_2}(\mathbf{r})|^2 \Psi_{\mathbf{n}_0, \mathbf{p}_3}^*(\mathbf{r}') \Psi_{\mathbf{n}_0, \mathbf{p}_3}(\mathbf{r}) \right], \quad (18)$$

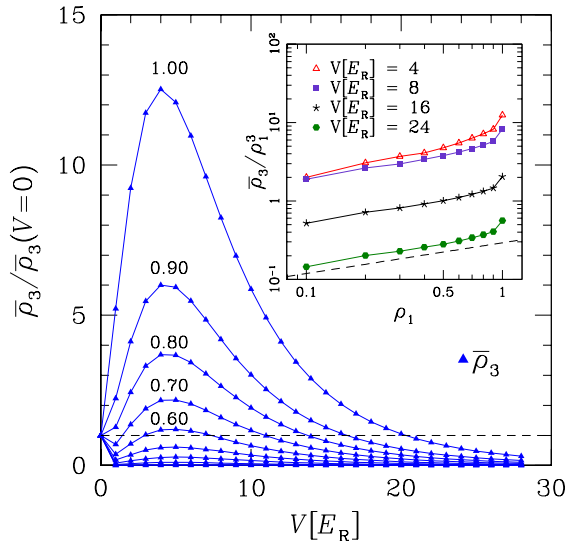


FIG. 3: (Color online) Averaged three-particle density $\bar{\rho}_3(V)$ via Eq. (16) as a function of the optical potential depth V for $R = a/2$. The graphs are normalized in such a way that $\bar{\rho}_3(V=0) = 1$ (free fermion gas). The data are for a partially filled lowest band in the ground state. The three-particle density decreases monotonically when the filling factor $\rho_1 = N_0/(2N^3)$ is decreased (data for $\rho_1 = 0.1, 0.2, 0.3, \dots, 1.0$). This shows that three-particle processes are suppressed when moving away from the band-insulating regime. The inset shows a log-log plot of the averaged three-particle density divided by ρ_1^3 , $\bar{\rho}_3(V)/\rho_1^3$, as a function of the filling factor ρ_1 for different values of the dimensionless potential depth V . For all V , $\bar{\rho}_3(V)/\rho_1^3$ decays according to a power law in ρ_1 . The dashed line in the inset is a guide to the eye proportional to $\rho_1^{0.391}$. The data shown are for $a = 1$ and $N = 65$.

where the characteristic function χ_Λ is

$$\chi_\Lambda(\mathbf{p}) \equiv \begin{cases} 1, & \mathbf{p} \in \Lambda, \\ 0 & \text{otherwise.} \end{cases} \quad (19)$$

In Fig. 3 the averaged three-particle density for a partially filled lowest band is plotted as a function of the potential strength V for several filling fractions $\rho_1 = N_0/(2N^3)$, where $\rho_1 = 1$ for a completely filled lowest band. For all values of V , the three-particle density decreases with a power-law behavior in ρ_1 (inset of Fig. 3), thus showing that in parabolic traps three-body processes can be suppressed in partially filled lowest bands due to the reduced filling of the lattice.

III. THERMOMETRY AND EFFECTS OF FINITE TEMPERATURES

In order to obtain a realistic estimate of the molecule formation rate, as well as the lifting of fermions into higher bands (cf. Sec. IV) the effects of finite temperatures must be taken into account. We start from a tight-binding-like Hamiltonian for the fermions,

$$\mathcal{H} = -t \sum_{\langle ij \rangle} (c_{i,\sigma} c_{j,\sigma}^\dagger + \text{c.c.}) + \frac{K}{2} \sum_j \mathbf{r}_j^2 n_{j,\sigma}, \quad (20)$$

where the optical lattice potential is quadratic ($\mathbf{r}^2 = x^2 + y^2 + z^2$) in units of $\lambda/2$ and $n_{j,\sigma} = c_{j,\sigma}^\dagger c_{j,\sigma}$ is the number operator.

Using experimentally relevant parameters [16] for the trap frequencies, $\omega_x = 2\pi \times 211$ Hz, $\omega_y = 2\pi \times 257$ Hz, $\omega_z = 2\pi \times 257$ Hz, which corresponds to a potential depth of $V[E_R] = 15.64$, we obtain $t/E_R = 0.00652$ [22], $K_z/E_R = 0.00411$, and $K_x/E_R = K_y/E_R = 0.00609$. We find that a system of size 100^3 is large enough to ensure that the particle density is zero at the edges. For a given temperature in units of the Fermi energy E_F , we tune the chemical potential such that for $T = 0$, as well as for a given $T > 0$, we obtain 40000 particles in the trap [16].

The fraction d_2 of double-occupied sites is given by

$$d_2 = \frac{\sum_j \langle n_{j,\uparrow} n_{j,\downarrow} \rangle}{\sum_j \langle n_{j,\uparrow} \rangle} = \frac{\sum_j \langle n_{j,\uparrow} \rangle \langle n_{j,\downarrow} \rangle}{\sum_j \langle n_{j,\uparrow} \rangle}. \quad (21)$$

Here $n_{j,\sigma}$ is the number operator for particles with spin σ . The second equality in Eq. (21) follows from the fact that the particles are noninteracting. Using $\rho_j = \langle n_{j,\sigma} \rangle$ for the expectation value of the number operator we obtain

$$d_2 = \frac{\sum_j \rho_j^2}{\sum_j \rho_j}. \quad (22)$$

Data for d_2 as a function of temperature T are shown in Fig. 4 for the experimental parameters used in Ref. [16]. Empirically we determine for several sets of experimental parameters that in the band-insulating regime for low temperatures and $V \gtrsim 5$

$$d_2 \approx a + b \exp(-\gamma T), \quad (23)$$

where the temperature is measured in units of the Fermi energy E_F . Note that for larger V we obtain $a = 0$ and $b = 1$ in Eq. (23), i.e., $d_2 \approx \exp(-\gamma T)$. This can be seen

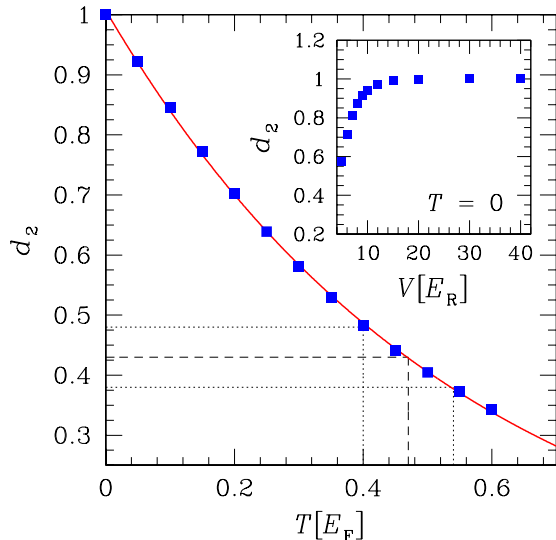


FIG. 4: (Color online) Fraction of double-occupied sites in an optical lattice of size 100^3 with 40000 particles for the experimental parameters presented in Ref. [16]. The temperature is measured in units of the Fermi energy E_F . The fraction of double-occupied sites decays exponentially with increasing temperature. In the experiments of Köhl *et al.* [16] $d_2 = 0.43 \pm 0.05$ (dashed \pm dotted lines). This means that the experiment is done at $T/E_F \approx 0.47 \pm 0.07$, which is considerably hotter than expected. The inset shows the fraction of double-occupied sites as a function of the potential depth at $T = 0$.

in the inset to Fig. 4: for deep lattices, i.e., $V \rightarrow \infty$, we obtain $d_2(T = 0) \rightarrow 1$ (data for 40000 particles and the experimental parameters used above). For the experimental parameters of Köhl *et al.*, we find $\gamma = 1.818$ ($a = 0, b = 1$) for $0 \leq T/E_F \leq 0.65$. Because the double occupancy depends only on the Fermi distribution and the density of states (which in turn depends on the space dimension), we expect the functional form to be independent of the trap parameters and only to depend on the space dimension of the lattice (which affects the density of states). Thus the molecule formation rate can be used in experiments to determine the temperature of the system, something which previously has not been accessible experimentally. These, as well as similar results obtained experimentally by Stöferle *et al.* [18] show that current experiments with fermions in optical lattices are done at temperatures considerably higher than in the continuum (Fig. 4).

IV. RAMPING ACROSS A FESHBACH RESONANCE

A magnetic field tuned near a Feshbach resonance [23] can be used to vary the two-body s -wave scattering length a_0 between two particles in different spin states over a broad range which at low temperatures becomes

the only relevant quantity to describe interactions. Experimentally [16] the s -wave interaction is varied on a short time scale compared to the tunneling time between two adjacent potential wells. Thus, the system in the band insulator regime can be regarded as an array of decoupled harmonic potential wells. Therefore, in the presence of a magnetic field, a cell of the optical lattice with a completely filled lowest band is well described by a two-body problem in a harmonic potential with zero-range interaction, a problem that has been studied theoretically in different approximation schemes [24, 25, 26, 27].

The scenario considered by Köhl *et al.* [16] is to start with a completely filled lowest band at a certain external magnetic field B_i below the Feshbach resonance. By crossing the resonance with a given velocity (in the experiment the ramping velocity is determined by maximizing the molecule formation rate as a function of the ramping velocity) and ending at a final magnetic field B_f , the large variation of the scattering length a_0 causes an interaction-induced transition between Bloch bands, i.e., a fraction of fermions is transferred to higher bands. We can understand this problem theoretically by restricting it at first to two particles situated at \mathbf{r}_1 and \mathbf{r}_2 , and choosing B_i and B_f such that $a_0(B_i) = a_0(B_f) = 0$. The general solution to this two-body problem [24] is a wave function $\Theta(\mathbf{r}, \mathbf{R})$ expressed in center-of-mass $\mathbf{R} = (\mathbf{r}_1 + \mathbf{r}_2)/\sqrt{2}$ and relative coordinates $\mathbf{r} = (\mathbf{r}_1 - \mathbf{r}_2)/\sqrt{2}$. For a vanishing scattering length a_0 , the initial and final wave function $\Theta_{i/f}(\mathbf{r}, \mathbf{R})$ can be expressed as

$$\Theta_{i/f}(\mathbf{r}, \mathbf{R}) = \Phi_{\mathbf{n}_{i/f}}(\mathbf{R})\phi_{n_{i/f}}(\mathbf{r}), \quad (24)$$

where $\Phi_{\mathbf{n}}(\mathbf{R})$ is the harmonic oscillator eigenstate with quantum number $\mathbf{n} \in \mathbb{N}^3$ and

$$\phi_n(\mathbf{r}) = \pi^{-3/4} \left[L_n^{1/2}(0) \right]^{-1/2} e^{-\mathbf{r}^2/2} L_n^{1/2}(\mathbf{r}^2) \quad (25)$$

is the harmonic oscillator s -wave function with quantum number n given in terms of generalized Laguerre polynomials $L_n^{1/2}(r)$ [28]. The *relative* part of the wave function [cf. Eq. (24)], i.e., the oscillator s -wave function, is then shifted upward by *one* quantum number when crossing the Feshbach resonance:

$$n_i \rightarrow n_f = n_i + 1, \quad (26)$$

whereas the quantum number of the center-of-mass contribution \mathbf{n} remains unchanged.

In the following we briefly outline our calculations before elaborating on the details. We start by expressing the Bloch bands $\Psi_{\mathbf{n}, \mathbf{p}}$ around a potential minimum \mathbf{R} by a product of two localized Wannier states $W_{\mathbf{n}, \mathbf{R}}(\mathbf{r})$, i.e.,

$$W_{\mathbf{n}, \mathbf{R}}(\mathbf{r}) \equiv \frac{1}{N^{3/2}} \sum_{\mathbf{p}} e^{-i\mathbf{p} \cdot \mathbf{R}} \Psi_{\mathbf{n}, \mathbf{p}}(\mathbf{r}), \quad (27)$$

where the summation is performed over the N^3 momenta \mathbf{p} in the first Brillouin zone. While the Bloch states are

extended over the lattice, the Wannier functions peak at a given lattice site with weight in neighboring sites being exponentially suppressed. The rate of exponential decay of Wannier functions in one dimension for a given energy band is related to the energy gap between that particular band and any other band [29]. Although in one space dimension the energy bands can always be well separated by increasing the optical potential depth V , the situation in three dimensions is more complicated due to entangled energy bands. If there is level crossing it is not possible to construct localized wave functions from Bloch states from one of these bands alone [30]. In this case localization of the corresponding Wannier functions is still possible because the potential $V(\mathbf{r})$ allows for the wave functions to separate, i.e., $W_{\mathbf{n},\mathbf{R}}(\mathbf{r}) = w_{n_1,R_1}(x_1)w_{n_2,R_2}(x_2)w_{n_3,R_3}(x_3)$, where the single factors $w_{n_i,R_i}(x_i)$ can always be localized. Note that the calculations using Wannier functions are done with a cutoff in the Fourier expansion of $c = 6$. Convergence tests show that our results are approximately independent of the lattice size for $N \geq 65$, and we perform the following calculations for $N = 65$.

In a next step, the Wannier functions are approximated with harmonic oscillator eigenstates and are split into center of mass and relative parts. Each relative part of an element in this approximation is shifted upward by

a quantum number, i.e., $\phi_n(\mathbf{r}) \rightarrow \phi_{n+1}(\mathbf{r})$. The final shifted two-particle wave function after passing the Feshbach resonance is then transformed back to absolute coordinates where wave functions in different Bloch bands then mix. Applying this procedure to all sites in the lattice yields the final excited state of all $2N^3$ particles.

In second quantization, we first express the Bloch states in Wannier functions by means of a unitary transformation [inverse of Eq. (27)]:

$$\hat{f}_{\mathbf{n},\mathbf{p},s}^\dagger = \frac{1}{N^{3/2}} \sum_{\mathbf{R}} e^{i\mathbf{p}\cdot\mathbf{R}} \hat{w}_{\mathbf{n},\mathbf{R},s}^\dagger. \quad (28)$$

The operators $\hat{f}_{\mathbf{n},\mathbf{p},s}^\dagger$ and $\hat{w}_{\mathbf{n},\mathbf{R},s}^\dagger$ in Eq. (28) create a particle with spin s in a Bloch state $\Psi_{\mathbf{n},\mathbf{p}}(\mathbf{r})$ or Wannier state $W_{\mathbf{n},\mathbf{R}}(\mathbf{r})$, respectively, where \mathbf{R} denotes a site in the lattice. We next expand the Wannier states in harmonic oscillator wave functions, up to order o . Thus the particle number operator for a Bloch state $\Psi_{\mathbf{n},\mathbf{p}}(\mathbf{r})$ with spin s given by

$$\hat{f}_{\mathbf{n},\mathbf{p},s}^\dagger \hat{f}_{\mathbf{n},\mathbf{p},s} = \frac{1}{N^3} \sum_{\mathbf{R},\mathbf{R}'} e^{i\mathbf{p}\cdot(\mathbf{R}-\mathbf{R}')} \hat{w}_{\mathbf{n},\mathbf{R},s}^\dagger \hat{w}_{\mathbf{n},\mathbf{R}',s} \quad (29)$$

can be approximated as

$$\hat{f}_{\mathbf{n},\mathbf{p},s}^\dagger \hat{f}_{\mathbf{n},\mathbf{p},s} \approx \frac{1}{N^3} \sum_{\mathbf{R},\mathbf{R}'} e^{i\mathbf{p}\cdot(\mathbf{R}-\mathbf{R}')} \left\{ c_{\mathbf{n},\mathbf{n}}^2 \hat{a}_{\mathbf{n},\mathbf{R},s}^\dagger \hat{a}_{\mathbf{n},\mathbf{R},s} + \left[c_{\mathbf{n},\mathbf{n}} \hat{a}_{\mathbf{n},\mathbf{R},s}^\dagger \left(\sum_{\mathbf{w}} c_{\mathbf{n},\mathbf{n}+\mathbf{w}} \hat{a}_{\mathbf{n}+\mathbf{w},\mathbf{R}',s} \right) + \text{c.c.} \right] \right\}, \quad (30)$$

where $\hat{a}_{\mathbf{n},\mathbf{R},s}^\dagger$ ($\hat{a}_{\mathbf{n},\mathbf{R},s}$) creates (annihilates) a particle with spin s in the harmonic oscillator state $\Phi_{\mathbf{n}}(\mathbf{r} - \mathbf{R})$. Here $c_{\mathbf{n},\mathbf{k}} = \langle \Phi_{\mathbf{k}} | W_{\mathbf{n},\mathbf{0}} \rangle$ is the projection of the Wannier state $W_{\mathbf{n},\mathbf{0}}$ onto $\Phi_{\mathbf{k}}$ and $\mathbf{u} \in \{(\pm 2, 0, 0), (0, \pm 2, 0), (0, 0, \pm 2)\}$, provided that for the summations in Eq. (30) only \mathbf{u} are considered for which the components of $\mathbf{u} + \mathbf{n}$ are non-negative. Note that, because of the s -wave nature of the ground state, only harmonic oscillator wave functions with an *even* total order appear in this expansion.

To first order in the expansion in harmonic oscillator wave functions, only terms containing $c_{\mathbf{n},\mathbf{n}}c_{\mathbf{n},\mathbf{n}}$ are considered whereas in second order terms containing $c_{\mathbf{n},\mathbf{n}}c_{\mathbf{n},\mathbf{n}+\mathbf{u}}$ are added. In order to measure the quasimomentum distribution, one starts with the initial many-particle wave function

$$|\Psi_i\rangle \equiv \prod_{\mathbf{R}} \hat{w}_{\mathbf{n}_0,\mathbf{R},\uparrow}^\dagger \hat{w}_{\mathbf{n}_0,\mathbf{R},\downarrow}^\dagger |0\rangle \quad (31)$$

with $\mathbf{n}_0 = (0, 0, 0)$, where the single $\hat{w}_{\mathbf{n}_0,\mathbf{R},\uparrow}^\dagger \hat{w}_{\mathbf{n}_0,\mathbf{R},\downarrow}^\dagger$ can be expanded in first or second order (in harmonic oscillator functions) in analogy to the terms of the sum in Eq. (30). For a first- and second-order expansion in har-

monic oscillator states, the transformation to relative and center-of-mass motion coordinates can be expressed in a form that transforms back to normal coordinates after the increment of the s -wave functions. Starting from a ground state we obtain

$$|\Psi_f\rangle \equiv \prod_{\mathbf{R}} \hat{F}_{o,\mathbf{R}}^\dagger |0\rangle, \quad (32)$$

where $\hat{F}_{o,\mathbf{R}}^\dagger$ depends only on the site \mathbf{R} and the expansion order $o \in \{1, 2\}$. The lowest-order result is

$$\begin{aligned} \hat{F}_{1,\mathbf{R}}^\dagger &= -\frac{1}{\sqrt{3}} c_{\mathbf{n}_0,\mathbf{n}_0}^2 \left(\frac{1}{2} \hat{a}_{\mathbf{n}_0,\mathbf{R},\uparrow}^\dagger \hat{a}_{(0,0,2),\mathbf{R},\downarrow}^\dagger \right. \\ &\quad - \frac{1}{\sqrt{2}} \hat{a}_{(0,0,1),\mathbf{R},\uparrow}^\dagger \hat{a}_{(0,0,1),\mathbf{R},\downarrow}^\dagger + \frac{1}{2} \hat{a}_{(0,0,2),\mathbf{R},\uparrow}^\dagger \hat{a}_{\mathbf{n}_0,\mathbf{R},\downarrow}^\dagger \\ &\quad + \frac{1}{2} \hat{a}_{\mathbf{n}_0,\mathbf{R},\uparrow}^\dagger \hat{a}_{(0,2,0),\mathbf{R},\downarrow}^\dagger - \frac{1}{\sqrt{2}} \hat{a}_{(0,1,0),\mathbf{R},\uparrow}^\dagger \hat{a}_{(0,1,0),\mathbf{R},\downarrow}^\dagger \\ &\quad + \frac{1}{2} \hat{a}_{(0,2,0),\mathbf{R},\uparrow}^\dagger \hat{a}_{\mathbf{n}_0,\mathbf{R},\downarrow}^\dagger + \frac{1}{2} \hat{a}_{\mathbf{n}_0,\mathbf{R},\uparrow}^\dagger \hat{a}_{(2,0,0),\mathbf{R},\downarrow}^\dagger \\ &\quad \left. - \frac{1}{\sqrt{2}} \hat{a}_{(1,0,0),\mathbf{R},\uparrow}^\dagger \hat{a}_{(1,0,0),\mathbf{R},\downarrow}^\dagger + \frac{1}{2} \hat{a}_{(2,0,0),\mathbf{R},\uparrow}^\dagger \hat{a}_{\mathbf{n}_0,\mathbf{R},\downarrow}^\dagger \right), \end{aligned} \quad (33)$$

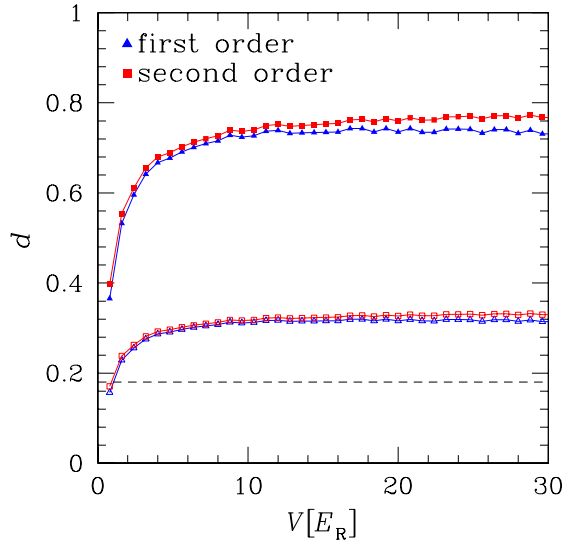


FIG. 5: (Color online) Upper set of curves: Fraction of fermions transferred to higher bands for a first- ($o = 1$) and second-order ($o = 2$) expansion [Eq. (35)] plotted as a function of the optical potential depth V in units of E_R . For both $o \in \{1, 2\}$, the fraction calculated in this work is nonvanishing, thus proving an interaction-induced transition between lowest bands, in qualitative agreement with results of Köhl *et al.* [16] (dashed line). The lower set of curves takes into account that, at finite temperatures, not all sites are double occupied. Using the parameters from Köhl *et al.* we expect $T \approx 0.47E_F$. The small discrepancy with the experimental data can be explained due to the parabolic trapping potential (see Sec. II C).

and the more complex higher-order expression $\hat{F}_{2,\mathbf{R}}^\dagger$ is omitted for the sake of brevity. Note that the quantum numbers of the creation and annihilation operators for harmonic oscillator states ($a^{(\dagger)}$) for each term always add to an even number because of the s -wave nature of the local wave functions.

The transformed multiparticle wave function Eq. (32) can now be used for the quasimomentum measurement

$$\hat{N}(o, \mathbf{n}, \mathbf{p}) \equiv \frac{1}{2} \langle \Psi_f | \hat{f}_{\mathbf{n},\mathbf{p},\uparrow}^\dagger \hat{f}_{\mathbf{n},\mathbf{p},\uparrow} + \hat{f}_{\mathbf{n},\mathbf{p},\downarrow}^\dagger \hat{f}_{\mathbf{n},\mathbf{p},\downarrow} | \Psi_f \rangle, \quad (34)$$

where the particle number operator $\hat{f}_{\mathbf{n},\mathbf{p},s}^\dagger \hat{f}_{\mathbf{n},\mathbf{p},s}$ from Eq. (30) is also considered in order o . For a first- and second-order expansion in terms of harmonic oscillator eigenstates, the calculation of the quasimomentum distribution is carried out analytically and the corresponding fraction of particles transferred to higher bands is defined as

$$d = \frac{\sum_{\mathbf{n} \neq \mathbf{n}_0} \sum_{\mathbf{p} \in 1^{st} \text{BZ}} \hat{N}(o, \mathbf{n}, \mathbf{p})}{\sum_{\mathbf{n}} \sum_{\mathbf{p} \in 1^{st} \text{BZ}} \hat{N}(o, \mathbf{n}, \mathbf{p})} \quad (35)$$

where the summation over the index \mathbf{n} is carried out over \mathbb{N}_0^3 .

In Fig. 5 the fraction of particles transferred to higher bands from Eq. (35) is plotted as a function of the optical potential depth V for a calculation in first- ($o = 1$) and second-order ($o = 2$) expansion. Our results show that already for $V[E_R] \sim 15$ the data have converged to the limit of a deep lattice. Over the whole range of the potential depth and for both orders, the fraction is nonvanishing, thus proving an interaction-induced transition between lowest bands in qualitative agreement with the results of Köhl *et al.* [16]. Note that while the relative part of the harmonic oscillator wave functions is lifted to the first band, this is *not* the case for the particles in the lattice. In the limit of deep lattices we find that [see Eq. (33)] only 75% of the particles are lifted: 50% into the first band and 25% into the second band, while the rest remain in the ground state. Finally, in Fig. 6 the quasimomentum distribution $\hat{N}(o, \mathbf{n}, \mathbf{p})$ from Eq. (34) with $o = 2$ is plotted in an extended zone scheme before (left panel) and after (center panel) ramping across the Feshbach resonance in comparison to the experimental results of Köhl *et al.* [16] after crossing the resonance (right panel). The numerical data are for zero temperature and illustrate how higher bands are populated when crossing the resonance. In Fig. 7 we show the quasimomentum distribution in an extended zone scheme plot at $T/E_F = 0.47$ before (left panel) and after (right panel) crossing the resonance. The data after crossing the resonance have been computed by taking into account that at $T/E_F = 0.47$ (the temperature used in the experiments of Köhl *et al.* [16]) only 43% of the sites are double occupied in the first Brillouin zone. In addition, higher-order zones are populated due to thermal fluctuations. The theoretical and experimental data agree well. Note that Köhl *et al.* used a trap with direction-dependent frequencies, which is why the quasimomentum distribution does not possess fourfold symmetry.

V. CONCLUSIONS

Fermionic systems in optical lattices show rich physical phenomena, and the physics of strongly interacting models is far from being understood. Before cold fermionic gases in optical lattices can be used as quantum simulators [1, 13, 14, 15], the agreement between experimental measurements and theoretical results has to be carefully checked for solvable models such as the ones discussed in this paper. One important issue is to ensure that the temperatures at which the experiments are performed truly probe the ground-state properties that are desired in a quantum simulation.

The calculations presented here for large three-dimensional fermionic systems rely on the fact that in experiments [16, 17, 18], the initial and final states of the fermions are essentially noninteracting. Strong interactions are present [19] only during the short ramping periods, and the effect of the interaction could be considered locally on the few-body states at each lattice site.

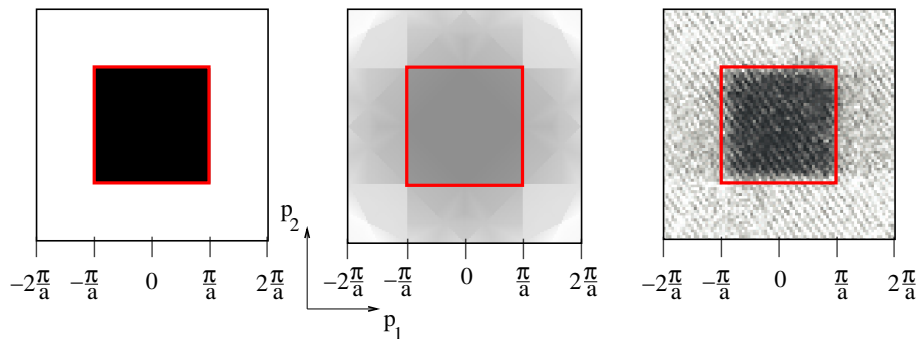


FIG. 6: (Color online) Quasimomentum distribution in the (p_1, p_2) plane, integrated over the third component p_3 at $T = 0$. Left: Momentum distribution before ramping across the Feshbach resonance. The first Brillouin zone (black box) is filled. Center: Numerical calculation in second order, showing the momentum distribution after crossing the Feshbach resonance. Data for a potential depth $V[E_R] = 40$ at which the sets of entangled energy bands are well separated from each other to avoid crossovers. The numerical data shown are for $a = 1$ and $N = 65$. Right: Experimental data taken from Köhl *et al* [16]. Note that in the experiment the optical lattice is turned off before the quasimomentum is measured.

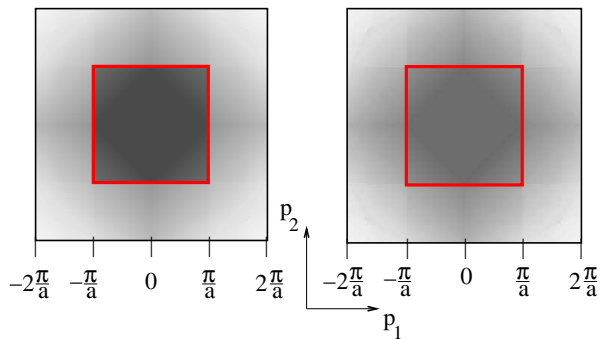


FIG. 7: (Color online) Quasimomentum distribution in the (p_1, p_2) plane, integrated over the third component p_3 at $T \approx 0.47E_F$, the temperature used in the experiments of Köhl *et al.* [16] (i.e., $d_2 = 0.43$). Left: Momentum distribution before ramping across the Feshbach resonance. Right: Numerical calculation in second order, showing the momentum distribution after crossing the Feshbach resonance, taking into account thermal effects.

In order to explain the low molecule formation rates observed in experiments, we have computed the two- and three-particle densities for fermions in optical lattices. In general, one would expect that the three-particle density decreases in a lattice system. Our results show that non-trivial processes occur when placing a fermionic gas in an optical lattice. First, the three-particle density *increases* with increasing potential depth, since up to intermediate lattice depths the main effect of the lattice is not a localization of the particles on individual lattice sites, but rather the reduction of the effective volume accessible to the fermions. The reduced volume leads to a higher fermion density at the lattice sites, and hence to larger three-particle densities and scattering. This increase of three-particle densities, which happens for experimentally relevant potential depths, provides an explanation, besides ramping speeds and imaging quality,

why the molecule formation rates and lifetimes in experiments [16] are lower than expected. The three-particle density decreases only for very deep lattices, when the Wannier functions become strongly localized on single lattice sites and three-body processes should not influence the experiments already for $V[E_E] \gtrsim 30$ [16].

Our calculations show that the fraction of double-occupied sites in the optical lattice varies approximately exponentially with the temperature. While the direct determination of the temperature of an experimental setup has proven to be difficult as well as inaccurate, the counting of particles can be done to good precision [18], and therefore the fraction of double-occupied sites can be determined. Our results provide a theoretical foundation to recent experimental work by Stöferle *et al.* [18] in which the molecule fraction can be used for thermometry in experiments, something that was previously not available for fermions in optical lattices. In particular, our results using standard experimental parameters show that experiments are currently performed in a temperature regime considerably hotter than for systems in the continuum. It is furthermore important to perform these measurements in deep lattices, as otherwise increased three-body scattering processes can influence the molecule formation.

When tuning the system across a Feshbach resonance by increasing the field and thus pushing fermions into higher bands we find good quantitative agreement between our results and the experiments of Köhl *et al.* [16].

Acknowledgments

We would like to thank T. Esslinger, M. Köhl, Wei Ku, H. Moritz, and S. D. Huber for discussions as well as K. Tran for carefully reading the manuscript. Part of the simulations were done on the Hreidar cluster at ETH

Zürich.

-
- [1] D. Jaksch, C. Bruder, J. I. Cirac, C. W. Gardiner, and P. Zoller, *Cold Bosonic Atoms in Optical Lattices*, Phys. Rev. Lett. **81**, 3108 (1998).
- [2] M. Greiner, O. Mandel, T. Esslinger, T. W. Hänsch, and I. Bloch, *Quantum phase transition from a superfluid to a Mott insulator in a gas of ultracold atoms*, Nature **415**, 39 (2002).
- [3] B. Paredes, A. Widera, V. Murg, O. Mandel, S. Fölling, I. Cirac, G. V. Shlyapnikov, T. W. Hänsch, and I. Bloch, *Tonks-Girardeau gas of ultracold atoms in an optical lattice*, Nature **429**, 277 (2004).
- [4] T. Stöferle, H. Moritz, C. Schori, M. Köhl, and T. Esslinger, *Transition from a Strongly Interacting 1D Superfluid to a Mott Insulator*, Phys. Rev. Lett. **92**, 130403 (2004).
- [5] G. G. Batrouni, V. Rousseau, R. T. Scalettar, M. Rigol, A. Muramatsu, P. J. H. Denteneer, and M. Troyer, *Mott Domains of Bosons Confined on Optical Lattices*, Phys. Rev. Lett. **89**, 117203 (2002).
- [6] V. A. Kashurnikov, N. V. Prokof'ev, and B. V. Svistunov, *Revealing the superfluid-Mott-insulator transition in an optical lattice*, Phys. Rev. A **66**, 031601 (R) (2002).
- [7] S. Wessel, F. Alet, M. Troyer, and G. G. Batrouni, *Quantum Monte Carlo simulations of confined bosonic atoms in optical lattices*, Phys. Rev. A **70**, 053615 (2004).
- [8] L. Pollet, S. M. Rombouts, and P. J. Denteneer, *Ultracold Atoms in One-Dimensional Optical Lattices Approaching the Tonks-Girardeau Regime*, Phys. Rev. Lett. **93**, 210401 (2004).
- [9] M. Rigol and A. Muramatsu, *Quantum Monte Carlo study of confined fermions in one-dimensional optical lattices*, Phys. Rev. A **69**, 053612 (2004).
- [10] C. Kollath, U. Schollwöck, J. von Delft, and W. Zwerger, *Spatial correlations of trapped one-dimensional bosons in an optical lattice*, Phys. Rev. A **69**, 031601(R) (2004).
- [11] H. P. Büchler, M. Hermele, S. D. Huber, M. P. A. Fisher, and P. Zoller, *Atomic quantum simulator for lattice gauge theories and ring exchange models*, Phys. Rev. Lett. **95**, 040402 (2005).
- [12] M. Troyer and U. Wiese, *Computational Complexity and Fundamental Limitations to Fermionic Quantum Monte Carlo Simulations*, Phys. Rev. Lett. **94**, 170201 (2005).
- [13] W. Hofstetter, J. I. Cirac, P. Zoller, E. Demler, and M. D. Lukin, *High-Temperature Superfluidity of Fermionic Atoms in Optical Lattices*, Phys. Rev. Lett. **89**, 220407 (2002).
- [14] C. Honerkamp and W. Hofstetter, *Ultracold Fermions and the $SU(N)$ Hubbard Model*, Phys. Rev. Lett. **92**, 170403 (2004).
- [15] S. Trebst, U. Schollwöck, M. Troyer, and P. Zoller, *Adiabatic construction of d-wave resonating valence bond states of ultracold fermionic atoms in optical lattices*, Phys. Rev. Lett. **96**, 250402 (2005).
- [16] M. Köhl, H. Moritz, T. Stöferle, K. Günter, and T. Esslinger, *Fermionic Atoms in a Three Dimensional Optical Lattice: Observing Fermi Surfaces, Dynamics, and Interactions*, Phys. Rev. Lett. **94**, 080403 (2005).
- [17] H. Moritz, T. Stöferle, K. Günter, M. Köhl, and T. Esslinger, *Confinement Induced Molecules in a 1D Fermi Gas*, Phys. Rev. Lett. **94**, 210401 (2005).
- [18] T. Stöferle, H. Moritz, K. Günter, M. Köhl, and T. Esslinger, *Molecules of Fermionic Atoms in an Optical Lattice*, Phys. Rev. Lett. **96**, 030401 (2006).
- [19] R. B. Diener and T. L. Ho, *Fermions in Optical Lattices across Feshbach Resonance*, Phys. Rev. Lett. **96**, 010402 (2005).
- [20] Note that a similar approach has been suggested by Pupillo *et al.* (see Ref. 31) for bosonic systems.
- [21] R. Grimm, M. Weidmüller, and Y. B. Ovchinnikov, *Optical dipole traps for neutral atoms*, Adv. At., Mol., Opt. Phys. **42**, 95 (2000).
- [22] W. Zwerger, *Mott-Hubbard transition of cold atoms in optical lattices*, J. Opt. B: Quantum Semiclassical Opt. **5**, 9 (2003).
- [23] C. J. Pethick and H. Smith, *Bose-Einstein Condensation in Dilute Gases* (Cambridge University Press, Cambridge, 2002).
- [24] T. Bush, B. G. Englert, K. Rzazewski, and M. Wilkens, *Two Cold Atoms in a Harmonic Trap*, Found. Phys. **28**, 549 (1998).
- [25] D. Blume and C. H. Greene, *Fermi pseudopotential approximation: Two particles under external confinement*, Phys. Rev. A **65**, 043613 (2002).
- [26] E. L. Bolda, E. Tiesinga, and P. S. Julienne, *Effective-scattering-length model of ultracold atomic collisions and Feshbach resonances in tight harmonic traps*, Phys. Rev. A **66**, 013403 (2002).
- [27] D. B. Dickerscheid, U. Al Khawaja, D. van Oosten, and H. T. Stoof, *Feshbach resonances in an optical lattice*, Phys. Rev. A **71**, 043604 (2005).
- [28] M. Abramowitz and I. A. Stegun, *Handbook of Mathematical Functions with Formulas, Graphs, and Mathematical Tables* (Dover, New York, 1964).
- [29] W. Kohn, *Analytic Properties of Bloch Waves and Wannier Functions*, Phys. Rev. **115**, 809 (1959).
- [30] M. Marzari and D. Vanderbilt, *Maximally localized generalized Wannier functions for composite energy bands*, Phys. Rev. B **56**, 12847 (1997).
- [31] G. Pupillo, C. J. Williams, and N. V. Prokof'ev, *Effects of finite temperature on the Mott insulator state*, Phys. Rev. A **73**, 013408 (2006).